A Combined Statistical Shape Model of the Scalp and Skull of the Human Head

Femke Danckaers[1], Daniël Lacko[2], Stijn Verwulgen[2], Guido De Bruyne[2(✉)], Toon Huysmans[1], and Jan Sijbers[1]

[1] imec - Vision Lab, Department of Physics, Faculty of Sciences, University of Antwerp, Antwerp, Belgium
{Femke.Danckaers, Toon.Huysmans, Jan.Sijbers}@uantwerpen.be

[2] Department of Product Development, Faculty of Design Sciences, University of Antwerp, Antwerp, Belgium
{Daniel.Lacko, Stijn.Verwulgen, Guido.DeBruyne}@uantwerpen.be

Abstract. In this paper, we describe a framework to build a combined statistical shape model (SSM) of the outer surface of the scalp and the inner and outer surface of the skull of the human head. Such an SSM is a valuable tool when designing headgear, as it captures the variability of head geometry of a given population, enabling detailed analysis of the relation between the shape of the scalp and the skull. A combined SSM of the head may allow to work towards population based Finite Element (FE) models e.g. for safety and comfort predictions when wearing headgear. Therefore, a correspondence between the skull and scalp surfaces, originating from MRI scans, is determined using elastic surface registration. The combined SSM shown to be compact, to be able to generalize to unseen instances by adjusting the shape parameters and to be shape specific. Therefore, we can assure that, by adjusting the shape parameters, a broad range of realistic head shapes can be formed.

Keywords: Statistical shape model · Human head · Scalp · Skull · Headgear · SSM

1 Introduction

A statistical shape model (SSM) of the human head is a valuable tool to design headgear, because it captures the variability of head geometry of a population. SSMs are built from 3D scans of a population of shapes. Therefore, they contain much more information than traditional anthropometrical measurements. When designing headgear, SSMs can be employed for ergonomic optimization warranting an optimal fit of the product to the geometry of the head, for a target population [1].

Insight in 3D skin and bone thickness of the human head for specific populations may help to avoid local peak pressure on the head while wearing a helmet in future helmets. Additionally, it may enhance the accuracy of Finite Element (FE) models of the human head that aim at predicting brain damage. The soft tissue layer is expected to

D.N. Cassenti (ed.), *Advances in Human Factors in Simulation and Modeling*,
Advances in Intelligent Systems and Computing 591, DOI 10.1007/978-3-319-60591-3_49

be a contributing parameter in the kinematics of head movement during head impact to affect rotational acceleration and velocity of the human brain. The bone tissue layer is a contributing parameter in the prediction of linear acceleration of the human brain during head impact.

A combined SSM of the head may allow to work towards population based FE models for safety and comfort predictions when wearing headgear. Such an FE head model can be used in simulations, to predict the impact on the head in accidents that cause trauma injuries to determine regional responses [2–5]. Typical FE head models are based on one head shape or the average head, calculated from a population [6–8]. A typical example is the Strasbourg University Finite Element Head Model [9, 10]. This is a very detailed FE model of the human head, with many internal structures included, and based on a single skull. By building an FE model from an SSM, it is adjustable in shape [2, 11], what can lead to more accurate, customizable FE models. Such a statistical FE model is especially useful when designing helmets [5, 12], because the impact on the head in an accident can be studied on different shapes and sizes of human heads, and thus improve the biofidelic characteristics of current FE head models for impact.

Most SSMs of the head only describe the outer skin layer of the head and do not contain information about the thickness of the scalp and the skull [1, 13, 14], while this information is important for e.g. predicting local skin pressure on the head. Claes et al. [15] constructed a combined SSM of the face shape and soft tissue depths for forensic facial reconstruction on an unidentified person's skull. Their technique is labor-intensive, as the researchers had to place manually indicated anatomical landmarks on the surface and measure soft tissue depths at 52 locations.

In this paper, we describe a technique for building a combined SSM of the human head, more specifically, the outer surface of the scalp and the inner and outer surface of the skull. The paper is organized as follows. First, the segmentation of the 3D surfaces from the MRI scans is detailed. Second, the construction of a combined SSM is explained. Next, in the results section, the SSM is subject to quality tests to evaluate the model's compactness, generalizability and shape specificity. Finally, the results are discussed and a conclusion is formulated.

2 Methods

Scalp and skull surfaces are separately segmented from MRI datasets. A reference mesh (a uniformly resampled surface from the dataset) is constructed for the scalp and for the skull, and is registered to all input meshes of each layer, to obtain a homologous point-to-point correspondence. Next, an average mesh is calculated for both the scalp and skull and used as template to register the input scalp and skull meshes for the second time to prevent a biased result. Then, the registered scalp and skull of each subject are merged again.

A combined SSM is built using Principal Components Analysis (PCA) on the corresponded heads. In this SSM, the average surface and skull thickness, and the main variances are incorporated. The process is shown in Fig. 1.

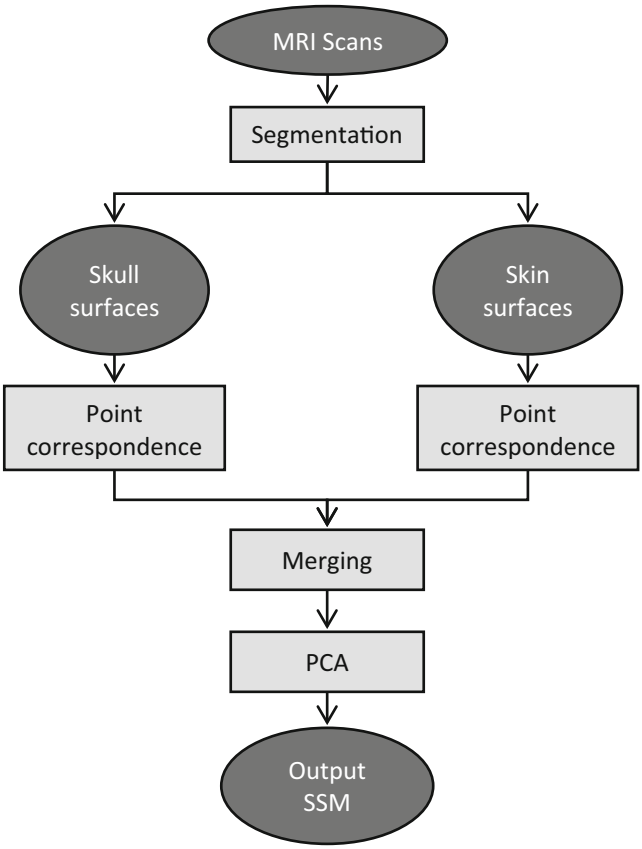

Fig. 1. Framework for building a combined SSM of the skull and scalp.

The training population consisted of 85 MRI T1-FFE-weighted scans (male and female, aged between 20 and 40 years, Western Population) originating from the International Consortium for Brain Mapping (ICBM) database [16]. The scans were acquired using a Philips ACS III 1.5 T scanner in the sagittal acquisition plane, with a slice thickness of 1 mm, an echo time of 10 ms, a repetition time of 18 ms and a flip angle of 30°.

2.1 Segmentation

From magnetic resonance imaging (MRI) scans, the scalp and the skull are separately segmented using the Statistical Parametric Mapping (SPM12) [17] package from MATLAB and converting the outcome to 3D meshes. The skin corresponds with layer 3 and the skull corresponds with layer 4 in SPM12. Scalp and skull were constructed separately by segmentation as different surfaces, because finding correspondences between nearby components is error-prone.

2.2 Statistical Shape Model (SSM)

In this section, the methodology to build a combined skull/scalp SSM is described. The algorithm is based on a previously developed elastic surface registration algorithm [18]. The first part of the framework is surface registration. The registered surfaces are used in the second part of the framework, where an SSM is built. The method is applicable to other layered surfaces as well.

Surface Registration. The first step of surface registration is a rigid alignment. Therefore, in both surfaces corresponding points are identified. This is done by casting a normal ray from each vertex of the reference surface to the target surface. When the normal of an intersection point is in the same direction (within a tolerance) as the normal of the point on the reference surface, that point can be considered corresponding. Another restriction for corresponding points is that the normal may not intersect the surface multiple times before reaching the corresponding point. The corresponding points serve as landmarks for a least-squares rigid alignment step.

In the elastic part of the registration the vertices are allowed to translate separately, while motion is restricted by a stiffness parameter that regulates the strength of the connection with the neighboring vertices and which decreases throughout the iterations. In this way, the movement of neighboring vertices is constrained, resulting in similar movements for nearby vertices. By applying weights to each vertex, the importance of this vertex can be set. If a corresponding point is found, its weight is set to 1.0. If no corresponding point for a vertex of the target mesh can be found, its weight is set to zero. In that case, this vertex simply translates along with its neighboring vertices.

Building a Statistical Shape Model. In the second part of our framework, an SSM is built based on the correspondences of N shapes, with every shape consisting of n vertices, that resulted from the surface registration [19]. To build an SSM, it is important that the surfaces are superimposed by optimally translating and rotating the surfaces to minimize the distance between corresponding points. In this way, shape information is maximally compressed. The optimal poses are determined by Procrustes analysis. The SSM is built by performing principal components analysis (PCA) on the corresponding points of the population.

In this SSM, the mean surface $\bar{\boldsymbol{x}} \in \mathbb{R}^{3n}$ and the main variances or PC modes, represented by $\boldsymbol{P} \in \mathbb{R}^{3n\times(N-1)}$, are incorporated. The population of N shapes is represented by an $3n$-dimensional point cloud, where each point represents a shape as a $3n$-dimensional vector of vertices. This cloud can be represented by $N-1$ eigenmode vectors, where the first eigenmode is the largest variance in the population, the second eigenmode is the second largest variance perpendicular to the first, etc. This means that a new surface vector $\boldsymbol{y} \in \mathbb{R}^{3n}$ can be formed by adapting the SSM parameters as follows

$$\boldsymbol{y} = \bar{\boldsymbol{x}} + \boldsymbol{P}\boldsymbol{b}, \tag{1}$$

with $\boldsymbol{b} \in \mathbb{R}^{(N-1)}$ the vector which contains the SSM parameters.

3 Experiments and Results

In this section, the results of the framework are described.

3.1 Segmentation

In the dataset, none of the skulls were completely segmented, because the SPM12 package was constructed with a focus on brain mapping and works with a spatially limited skull template. The dataset was sufficient for our research, because we work on comfort of helmets and therefore focus on the upper part of the head. A slice of the head of a test subject and the resulting skull and scalp surfaces are shown in Fig. 2. Note that in some scans a bar is visible on the top of the head, because the heads of the subjects from the ICBM are fixated. This bar is not visible in the model, because a smooth template surface served as input for the elastic surface registration to reduce protrusions and other irregularities. Remaining irregularities were averaged out by calculating the SSM.

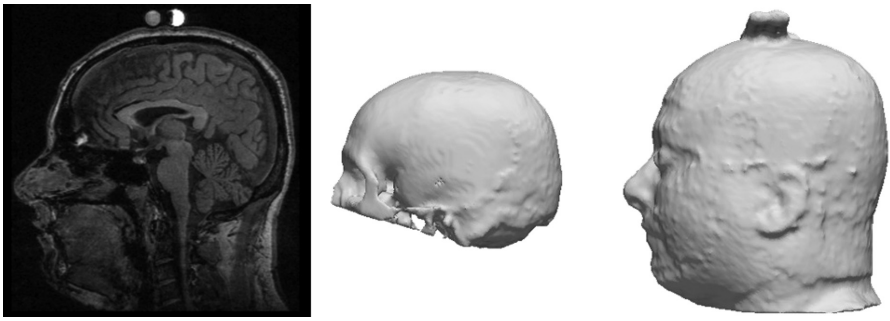

Fig. 2. Slice of a head scan and a segmented scalp and skull. Note that the skull is not fully segmented, because SPM12 focuses on the brain. A bar is noticeable on the top of the head.

3.2 Statistical Shape Model (SSM)

The scalp and the skull were separately segmented from each head scan, and were both registered by the same template surfaces. The skull template surface was uniformly resampled to 100041 vertices, the scalp template surface was uniformly resampled to 89389 vertices. After the surface registration, both scalp and skull of the same subject were merged to become a combined surface, as shown in Fig. 3.

In Fig. 4, the first three PC modes of the SSM, built from combined surfaces, are shown. These shape modes describe the shape variations inside the population. The first mode describes mainly the size of the head, the second mode describes the width-length ratio of the head, and the third mode describes mainly the curvedness of the skull.

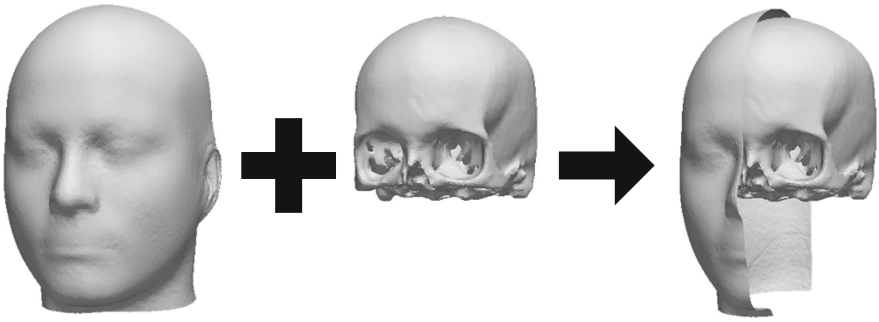

Fig. 3. Uniting the separate skull and scalp from Fig. 2 to result in a combined surface.

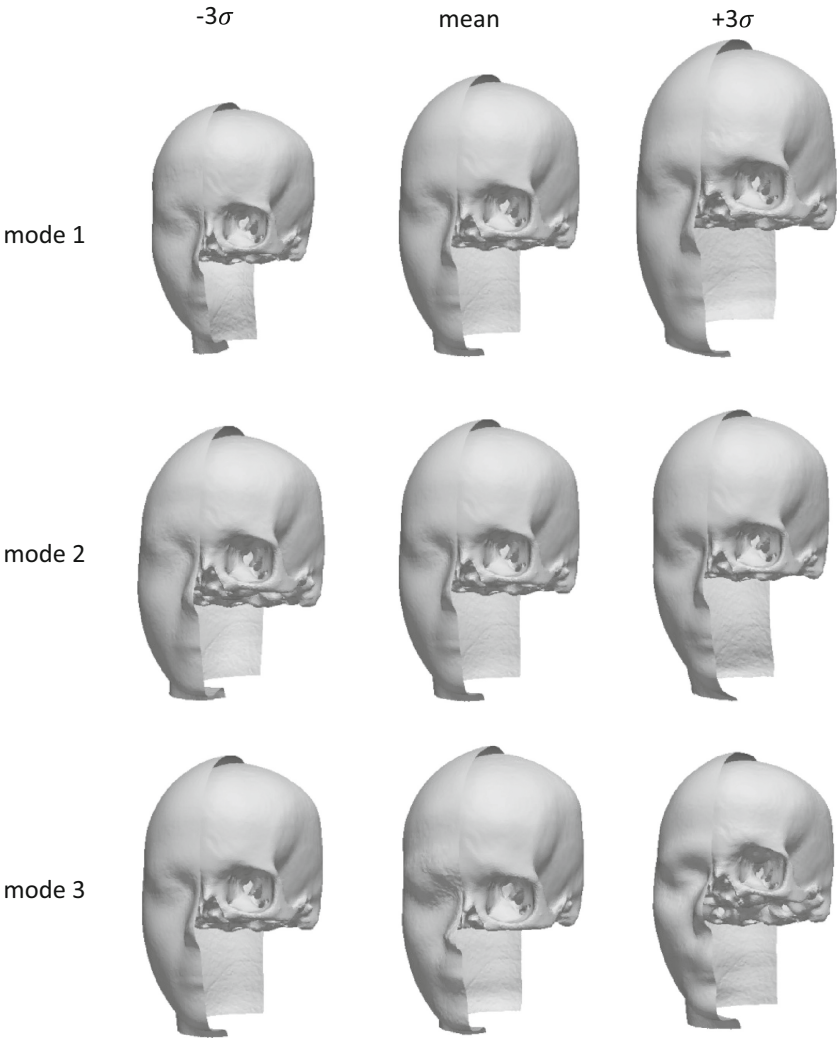

Fig. 4. First three eigenmodes of the combined SSM of the human scalp and skull.

3.3 Model Performance

Compactness, generalization ability, and specificity are widely used measures [20, 21] for quantifying the correspondence quality of an SSM. In this section, the different model performance measures were calculated for the combined SSM and the separate SSMs of the skull and the head.

Compactness. Compactness of a shape model is a measure how well a shape from the population is described by a limited amount of PC modes. Preferably, an SSM is approximated well with few modes. The compactness is expressed as the sum of variances of the SSM:

$$C(m) = \sum_{i=1}^{m} \lambda_i, \tag{2}$$

where λ_i is the variance on the vertex locations in shape mode i, and $C(m)$ is the compactness using m modes.

The results are shown in Fig. 5. To describe over 80% of the shape variation inside the population of combined head shapes, six shape modes were needed. Thirteen shape modes describe over 90% of the shape variation. Therefore, our combined SSM is a compact representation of the population.

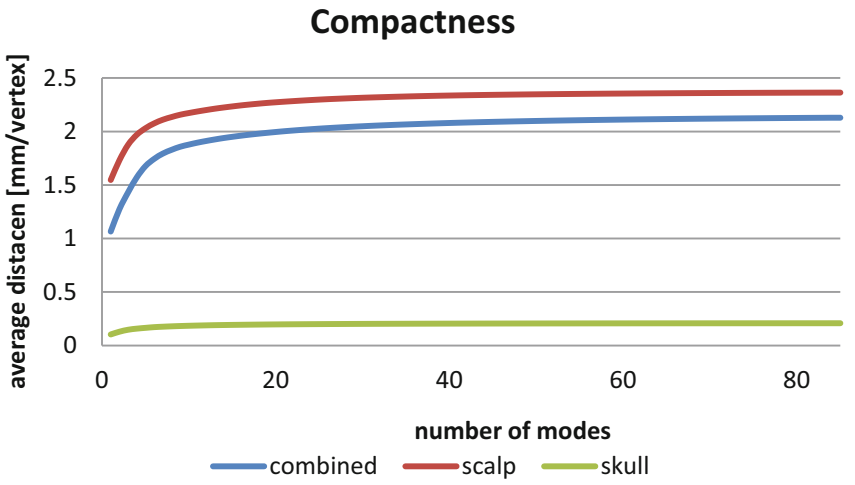

Fig. 5. Compactness graph. The average deviation from the mean shape to describe shapes with a specific number of shape modes is shown.

An example of a surface represented by different numbers of modes is shown in Fig. 6. Using more parameters led to a shape that looked more like the original shape. The more parameters that are used to reconstruct a shape, the less difference is noticeable.

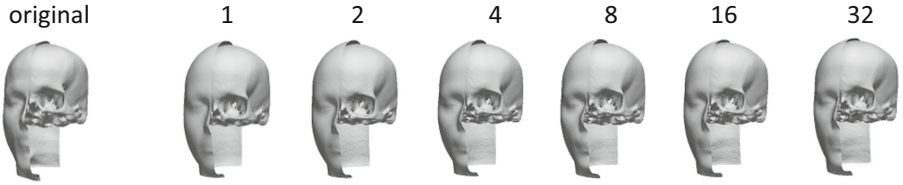

Fig. 6. Shape generated with a different number of shape modes. Note the difference in shape of the cheekbones and jaw. The difference between a surface reconstructed by 16 shape modes and 32 shape modes is minimal.

Generalizability. Generalizability relates to how well the SSM can generalize to a formerly unseen head shape. The SSM should be able to describe all head shapes, not only the head shapes of the training set. If an SSM is over-fitted to the training set, it will not be able to generalize to unseen samples.

Generalizability $G(m)$ was measured by performing leave-one-out tests, where an SSM was built by using all training shapes but one. Next, the left-out shape was described by adapting the shape parameters of the SSM. Generalizability was calculated as the mean error over all left out shapes,

$$G(m) = \frac{1}{N_m} \sum_{i=1}^{m} \|\boldsymbol{x}_i - \boldsymbol{x}_i'(m)\|^2, \tag{3}$$

where $\boldsymbol{x}_i$ is the left out shape and $\boldsymbol{x}_i'(m)$ is the attempted description using the SSM with m modes. The number of trials, or objects in the SSM, is represented by N_m.

In Fig. 7, the generalizability graph is shown. The generalizability error was calculated in mm per vertex. The error of fitting a scalp and skull to an unseen instance

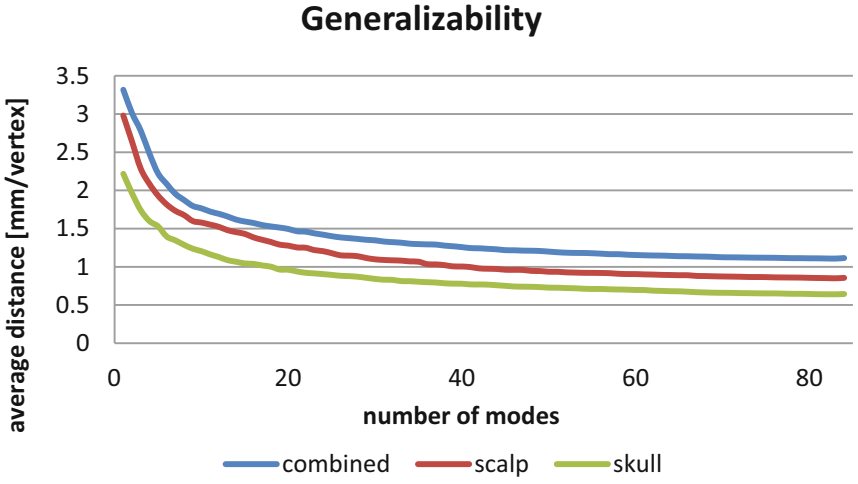

Fig. 7. The generalizability measure, in mm per vertex. The error flags represent the standard errors on the mean distance.

was 2.2 mm from five shape modes. Using 20 shape modes, the error was smaller than 1.5 mm. Note that the error for the scalp and skull separately was smaller than the error of the merged surface. This can be explained by the fact that the shape of both scalp and skull were dependent on each other. In future work, we will improve this by corresponding the scalp and skull together instead of corresponding them separately.

Specificity. A specific SSM can only represent instances of the object class that are similar to those in the training set. This was measured by generating an amount of shapes $(N_r = 1000)$ by generating a random parameter vector with m modes. Each sample was compared to the most similar shape in the training set. The specificity measure can be expressed as

$$G(m) = \frac{1}{N_m} \sum_{i=1}^{m} \|\boldsymbol{x}_i - \boldsymbol{x}_i'(m)\|^2, \tag{4}$$

with $\boldsymbol{x}_i'$ a shape example generated by the SSM and $\boldsymbol{x}_i$ the nearest member of the training set.

In Fig. 8, the specificity graph is shown. The specificity error was calculated in mm per vertex. The specificity test proved that our SSMs were able to generate shapes that resemble those in the training set, even though they differ from the shapes in the training set. The specificity error for the combined SSM is greater than the error for the separate SSMs. This means that the combined SSM represented more shape variation.

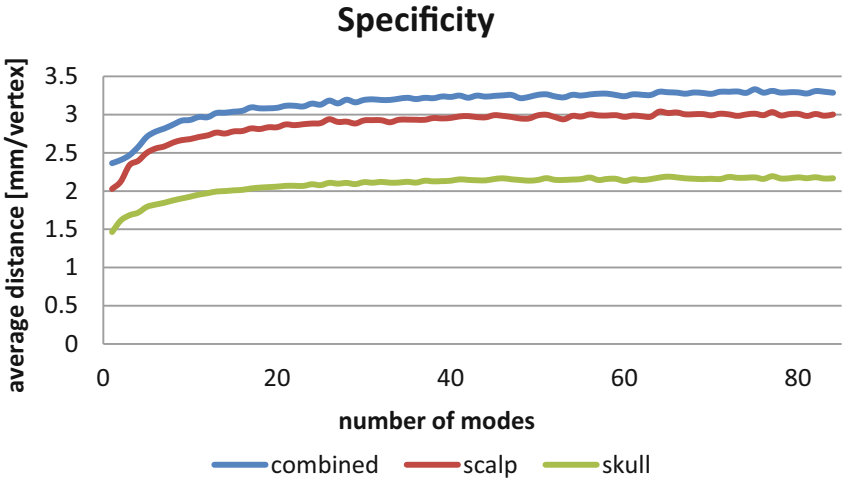

Fig. 8. The specificity measure, in mm per vertex. The error flags represent the standard errors on the mean distance.

4 Discussion

This combined SSM can be used as a virtual ergonomic 3D mannequin in Computer Aided Design (CAD) environments or as input for Finite Element (FE) and Computational Fluid Dynamics (CFD) simulations, when designing headgear. For example, it can be exploited in mass customization of all kinds of headgear systems that are built from FE models predicting local pressure. Another application is the development towards patient specific FE head impact models that may give more insight in brain damage due to accidents and can guide medical staff members during brain surgery.

The SSM is a compact representation of the population, because only six shape modes were needed to describe over 80% of the shape population. The model is able to generalize to an unseen instance, as six modes were sufficient to describe the instance with a mean error of 2.08 mm. A randomly generated shape using six shape modes is object specific, but differs from the dataset, since the average distance between a randomly generated object using six shape modes and the most similar object in the dataset was 2.77 mm. For helmet designing, a generalizability error of less than 1 mm is preferable. Our current model has a generalizability error of 1.1 mm when all shape modes are used to deform the model to an unseen head shape.

5 Conclusion and Further Work

In this work, we proposed a technique to perform statistical shape analysis on combined surfaces of the scalp and skull. Therefore, the relation between the scalp and skull can be analyzed. The constructed combined SSM is compact, so it can represent heads with a limited number of parameters with acceptable accuracy. Furthermore, we have proven that the combined SSM is able to generalize to unseen instances and is shape specific. Therefore, we can assure that by adjusting the shape parameters, a broad range of realistic head shapes can be formed. Our presented method is also applicable to other layered shapes.

The correspondences in the current SSM were split up in a skull part and a scalp part and merged for building a PCA model. For future work, we envision corresponding the combined surfaces, to assure a better correlation between skull and scalp.

Acknowledgements. This work was supported by the Agency for Innovation by Science and Technology in Flanders (IWT-SB 141520 and IWT 140881).

References

1. Lacko, D., et al.: Evaluation of an anthropometric shape model of the human scalp. Appl. Ergon. **48**, 70–85 (2015)
2. Bredbenner, T.L., Eliason, T.D., Francis, W.L., McFarland, J.M., Merkle, A.C., Nicolella, D.P.: Development and validation of a statistical shape modeling-based finite element model of the cervical spine under low-level multiple direction loading conditions. Front. Bioeng. Biotechnol. **2**(November), 58 (2014)

3. Jacob, A., et al.: Evaluation of helmet protection during impact of head to ground and impact of an object to head using finite element analysis. J. Saf. Eng. **5**(1), 8–16 (2016)
4. Mustafa, H., Pang, T.Y., Perret-Ellena, T., Subic, A.: Finite element bicycle helmet models development. Procedia Technol. **20**(July), 91–97 (2015)
5. Pintar, F.A., Philippens, M.M.G.M., Zhang, J., Yoganandan, N.: Methodology to determine skull bone and brain responses from ballistic helmet-to-head contact loading using experiments and finite element analysis. Med. Eng. Phys. **35**(11), 1682–1687 (2013)
6. Ponce, E., Ponce, D., Andresen, M.: Modeling heading in adult soccer players. IEEE Comput. Graph. Appl. **34**(5), 8–13 (2014)
7. Valdes-Hernandez, P.A., et al.: Approximate average head models for EEG source imaging. J. Neurosci. Methods **185**(1), 125–132 (2009)
8. Lei, Z., Yang, J.J., Zhuang, Z.: Headform and N95 filtering facepiece respirator interaction: contact pressure simulation and validation. J. Occup. Environ. Hyg. **9**(1), 46–58 (2012)
9. Asgharpour, Z., Baumgartner, D., Willinger, R., Graw, M., Peldschus, S.: The validation and application of a finite element human head model for frontal skull fracture analysis. J. Mech. Behav. Biomed. Mater. **33**, 16–23 (2014)
10. Tinard, V., Deck, C., Willinger, R.: New methodology for improvement of helmet performances during impacts with regards to biomechanical criteria. Mater. Des. **37**, 79–88 (2012)
11. Klein, K.F., Hu, J., Reed, M.P., Hoff, C.N., Rupp, J.D.: Development and validation of statistical models of femur geometry for use with parametric finite element models. Ann. Biomed. Eng. **43**(10), 2503–2514 (2015)
12. Zhang, L., Makwana, R., Sharma, S.: Brain response to primary blast wave using validated finite element models of human head and advanced combat helmet. Front. Neurol. **4**(August), 1–12 (2013)
13. Xi, P., Shu, C.: Consistent parameterization and statistical analysis of human head scans. Vis. Comput. **25**(9), 863–871 (2009)
14. Meunier, P., Shu, C., Xi, P.: Revealing the internal structure of human variability for design purposes. In: 17th World Congress on Ergonomics (2009)
15. Claes, P., Vandermeulen, D., De Greef, S., Willems, G., Suetens, P.: Craniofacial reconstruction using a combined statistical model of face shape and soft tissue depths: methodology and validation. Forensic Sci. Int. **159**, S147–S158 (2006)
16. Capetillo-Cunliffe, L.: Loni: Laboratory of Neuro Imaging (2007)
17. Kazemi, K., Noorizadeh, N.: Quantitative comparison of SPM, FSL, and brainsuite for brain MR image segmentation. J. Biomed. Phys. Eng. **4**, 13–26 (2014)
18. Danckaers, F., Huysmans, T., Lacko, D., Ledda, A., Verwulgen, S., Van Dongen, S., Sijbers, J.: Correspondence preserving elastic surface registration with shape model prior. In: Proceedings - International Conference on Pattern Recognition (2014)
19. Cootes, T.F., Taylor, C.J., Cooper, D.H., Graham, J.: Active shape models-their training and application. Comput. Vis. Image Underst. **61**(1), 38–59 (1995)
20. Davies, R.H., Twining, C.J., Cootes, T.F., Waterton, J.C., Taylor, C.J.: A minimum description length approach to statistical shape modeling. IEEE Trans. Med. Imaging **21**(5), 525–537 (2002)
21. Zihua, S.: Statistical Shape Modelling: Automatic Shape Model Building. University College London (2011)